

## **Pneumatic capillary gun for ballistic delivery of microparticles.**

Dmitry Rinberg

*Monell Chemical Senses Center, 3500 Market St., Philadelphia, PA 19104*

Claire Simonnet and Alex Groisman<sup>a)</sup>

*Department of Physics, University of California, San Diego, 9500 Gilman Drive, La Jolla, CA, 92093*

### **Abstract**

A pneumatic gun for ballistic delivery of microparticles to soft targets is proposed and demonstrated. The particles are accelerated by a high speed flow of Helium in a capillary tube. Vacuum suction applied to a concentric, larger diameter tube is used to completely divert the flow of Helium from the gun nozzle and prevent it from hitting the target. Depths of penetration of micron-sized gold particles into agarose gels and their speeds of ejection from the gun nozzle are measured.

---

<sup>a)</sup> Author to whom correspondence should be addressed; electronic mail: [agroisman@ucsd.edu](mailto:agroisman@ucsd.edu)

High density micron-size particles accelerated to high speeds can penetrate deep inside live tissues without inflicting much damage to the cells, and can be used to deliver genetic material to the cells they pierce<sup>1</sup>. This method of ballistic delivery is often called ‘biolistics’ and the device for shooting particles – ‘Gene Gun’. Biolistics proved to be an efficient method for delivery of plasmids and transfection of prokaryotic and eukaryotic (including mammalian) cells<sup>2,3</sup>. Recently it has been used for staining of neuronal tissue with fluorescent dyes<sup>4,5</sup>.

A modern version of the gene gun, Helios (Bio-Rad, Hercules, CA), uses ~1  $\mu\text{m}$  in diameter particles made of gold or tungsten, which are accelerated by a short pulse of a high speed flow of Helium. While the small holes in the cellular membranes along the particle tracks are normally quickly healed, the high speed jet of He emerging from the gun nozzle can produce severe damage to the tissue. In order to slow the flow of He, the nozzle expands towards the end, the target is usually shot from a significant distance, and sometimes a mesh filter is placed between the nozzle and the target<sup>5</sup>. Although there is little data on the actual speeds of the particles from the Helios Gene Gun, all those measures decelerate the particles and reduce their penetration depth. A major increase in the depth of penetration into an agarose gel (used to emulate a brain tissue) was reported with a more focused jet of He and short shooting distance, but it was accompanied by significant damage of the gel surface<sup>6</sup>. Large penetration depth and minimal damage would be very beneficial for staining and transfection of various live tissues, in particular mammalian brain where most of the cell bodies lie 100  $\mu\text{m}$  below the surface.

In this paper, we propose an alternative design of a pneumatic gun for ballistic particle delivery. Its key feature is the use of active vacuum suction to completely divert the high speed flow of the gas (He) from the gun nozzle, so that there is no damage to the target from the gas flow, Fig.1. The particles are accelerated by continuous high speed flow of He in the inner capillary tube, ICT. The suction is continuously applied through the outer capillary tube, OCT. The diversion occurs over a distance of less than 1 mm, on a time scale of ~2  $\mu\text{s}$  and is expected to have minimal effect on motion of the particles, which are much more inertial than the He gas.

ICT is made of polyamide coated fused silica (MicroFil™ Gauge 23, WPI Inc., Sarasota FL), has an inner diameter  $D_i = 530 \mu\text{m}$  and outer diameter of 665  $\mu\text{m}$ , and is glued to a plastic luer adapter (Fig.1). OCT is a piece of a stainless steel hypodermic tube with inner and outer diameters of 1.70 and 2.11 mm, respectively. It is made concentric with ICT by two 150  $\mu\text{m}$  thick “gears” (Fig.1). One end of OCT is hermetically glued to the luer adapter, and the other end is covered by a  $\varnothing 2.2$  mm circular cap with a  $\varnothing 150 \mu\text{m}$  opening in the middle. The cap is 50  $\mu\text{m}$  thick and has three 100  $\mu\text{m}$  tall pillars for mechanical strength and self-centering with OCT, to which it is glued (Fig.1). The cap and the gears are micro-machined out of UV-curable epoxy SU8 (MicroChem, Newton MA) using contact lithography<sup>7</sup>. The opening in the cap, ICT and OCT are coaxial within ~25  $\mu\text{m}$ . OCT is connected to vacuum through an ~1.5 mm opening in its side (at ~20 mm from the cap) and a plastic T-shaped barbed fitting, which is hermetically glued to OCT. We empirically found that the best results are achieved with a distance between the cap and the end of ICT in the range of 600-900  $\mu\text{m}$ . Four individual guns with distances in that range were tested, and their performance was virtually indistinguishable. The lengths of ICT,  $L_i$ , were 50-55 mm.

The gun was mounted vertically with the cap facing down and connected to a house vacuum system with a gauge pressure of -86 kPa. The luer adapter (and ICT inlet) was connected to a source of compressed He with adjustable pressure through two parallel lines of flexible Tygon tubing. The first line was always open, while the second was normally closed by a solenoid valve. The tubing downstream from the valve had a short detachable segment, where gold particles were loaded as a dry powder. The particles were “fired” by opening the valve for 300 ms, which created a flow of He through the second line, bringing the particles to ICT. The He pressure was set 1-2% below the point (about 120 kPa) where a directed stream of He emerging from the cap could be detected by appearance of ripples on surface of water in a Petri dish placed ~1 mm under the cap. We measured the volumetric flow rate of He through ICT,  $Q$ , by the rate of displacement of water from a graduated cylinder by the submerged gun with disconnected vacuum suction. That gave an estimate of the average flow rate at the outlet of ICT,  $\bar{v} = Q / (\pi D_i^2 / 4) \cong 630$  m/s. The impact of the flow of He through the cap onto the water surface in the Petri dish was less than that of a flow through ICT at 0.2 m/s without the vacuum suction.

To characterize the performance of the gun, we made test shots into agarose gels (N9302774, Applied Biosystems, CA), which are commonly used to emulate live tissues. We used three different types of spherical gold particles, that we call A, B and C, with respective diameters of  $0.47 \pm 0.15$ ,  $1.1 \pm 0.1$  and  $1.27 \pm 0.27$   $\mu\text{m}$  by BioRad (samples characterized under an electron microscope). The shots were made from a distance of 1 mm, and the gels were inspected under dark field illumination with a 50x/0.5 objective. Representative snapshots of a 3% gel shot with size B particles imaged at various depths into the gel are shown in Fig.2a-c. The particles near the plane of image are seen as sharp bright dots, while the out-of-focus particles contribute to the bright background. The diameter of the bright circle is ~150  $\mu\text{m}$ , which closely matches the opening in the cap. Figure 2.d-f shows images of the same type of particles and the same gel from a typical shot with a Helios gun, imaged at the same depths as Fig.2a-c. The shot was made at 175 psi from ~4 cm, which are typical settings for delivery of plasmids to cell cultures, and covered an area ~1.2 cm in diameter.

Examining the photographs in Fig.2b,c,e and f one can observe that unlike the Helios gun, the capillary gun delivers a notably larger number of particles to 55  $\mu\text{m}$  than to 35  $\mu\text{m}$  depth. The number of particles at different depths was counted by taking a stack of images with a step of 3  $\mu\text{m}$  in depth, with Image-Pro software (Media Cybernetics, Silver Spring, MD) to identify bright dots. The distributions of the three kinds of particles by depths for shots with the capillary gun and Helios gun at 175 and 120 psi are shown in Fig.3a-c. The latter pressure is the upper limit for staining delicate brain tissue. Each curve represents statistics on  $\sim 10^4$  and  $3\text{-}7 \cdot 10^4$  individual particles for the capillary and Helios Gene Gun, respectively. With the capillary gun, the mean penetration depths for particles A, B and C are 20, 39 and 38  $\mu\text{m}$ , respectively. With the Helios Gene Gun, the mean depths are 17, 36 and 39  $\mu\text{m}$  and 4.5, 32 and 48  $\mu\text{m}$  at 175 psi and 120 psi, respectively. Thus, penetration depths with the capillary gun are consistently larger for small particles, especially when it is important to minimize the impact of the gas jet on the target. Further, while the depth distributions for the Helios gun are very broad, the distributions for the capillary gun have peaks near the maximal penetration depths. The

peak is sharpest for the most monodisperse sample B; about 60% of the B particles are delivered to depths between 40 and 80  $\mu\text{m}$ .

We tried shooting with the capillary gun into 0.25 - 3% agarose gels, and no apparent damage of the gel surface (other than perforation by the particles) was detected in any of the tests. The particle penetration depth decreased with both shooting distance and agarose concentration, obviously due to viscous friction in air and higher resistance to particle motion in denser gels. Nevertheless, the depth distributions always had a peak near the maximal depth, and we assumed it was a counterpart of the peak in velocity distribution of particles reaching the gel surface. To learn more about the velocity at that peak,  $v_p$ , we plotted the depth at the peak,  $d$ , as a function of distance,  $h$ , between the cap and the gel surface for particles A, B and C, (inset in Fig.3). For higher resolution in  $d$ , we used a 0.25% gel, where the depth of penetration was largest. Dependence of  $d$  on  $h$  was close to a linear decay for all particle sizes, which is consistent with resistance being linear in velocity in both air and gel, and the gel resistance coefficients being higher by factors from 230 to 330.

The condition  $d = 0$  was met at  $h_0 = 10.8, 24$  and  $35$  mm for particles A, B and C, respectively (inset in Fig.3). We can estimate velocity at the peak of the distribution for particles emerging from the gun,  $v_0$ , if we assume that  $d = 0$  corresponds to  $v_p = 0$  and that the resistance force in the air follows Stokes' equation for a sphere,  $F = 6\pi r \eta_a v$ ,<sup>8</sup> where  $r$  is particle radius and  $\eta_a = 1.83 \cdot 10^{-5}$  Pa·s is air viscosity. Integrating the Stokes' equation we get  $v_0 = 6\pi r \eta_a h_0 / m = 9\eta_a h_0 / (2\rho_g r^2)$ , where  $m$  is the mass of a particle and  $\rho_g$  is density of gold. Plugging in the values of  $h_0$  and mean  $r^2$ , we obtain  $v_0 = 760, 340$  and  $360$  m/s for particles A, B and C. The calculated particle velocities are comparable with the speed of sound in air (343 m/s) and imply relatively high Reynolds numbers for particle motion  $Re_p = v_0 r \rho_a / \eta_a = 10-15$  ( $\rho_a = 1.20$  kg/m<sup>3</sup> is the density of air). To check applicability of the Stokes' law at those conditions we made test shots in He and H<sub>2</sub> atmospheres instead of air. The speeds of sound,  $v_s$ , in those gases are  $\sim 1000$  and  $1300$  m/s, the viscosities are  $\eta_{He} = 1.98 \cdot 10^{-5}$  and  $\eta_{H_2} = 0.89 \cdot 10^{-5}$  Pa·s, and the densities are  $0.165$  and  $0.082$  kg/m<sup>3</sup>, respectively. This implies lower  $Re_p$  and  $v_0/v_s$  ratios for both gases and twice lower viscous friction in H<sub>2</sub> than in air. Nevertheless, when the shooting distance  $h$  was multiplied by the viscosity ratio ( $\eta_{He}/\eta_a$  and  $\eta_{H_2}/\eta_a$ ), the measured values of  $d$  fell on the same curves as for air (Fig.4), in agreement with the Stokes' law.

It is instructive to compare the speeds of the particles with flow velocity of He in ICT. Because of compressibility of He, significant inertial effects ( $Re = \bar{v} D_i \rho_{He} / \eta_{He} \approx 2800$  and the Reynolds stress,  $\rho_{He} \bar{v}^2 / 2 \approx 33$  kPa), and changes in the flow profile with the distance from the inlet, the flow velocity is a complex function of position, even if the flow is laminar<sup>8,9</sup>. At the ICT inlet, where the absolute pressure is about 2.2 atm, the velocity of He,  $v_i$ , is estimated as  $\bar{v} / 2.2 \approx 300$  m/s. The outlet is a distance  $L_i \approx 0.035 D_i Re$  from the inlet, which implies a close to parabolic flow profile<sup>8,9</sup> with characteristic flow velocities within the central 150  $\mu\text{m}$  of ICT (from which the particles are ejected from the gun, Fig.1) of about  $1.8\bar{v} \approx 1100$  m/s<sup>8,9</sup>. The speed of type

A particles is comparable to that of He at the outlet, while the speeds of B and C particles are closer to that of He at the inlet. An apparent reason for this is the much greater characteristic length,  $L_a = v^2 / (F / m) = 2\rho_g v r^2 / (9\eta_{He})$ , required for a flow to accelerate larger particles. At  $v = 630$  m/s,  $L_a$  is only 7.5 mm for A particles, but it is 41 and 55 mm for B and C particles, which is comparable to  $L_i$ . Thus, the final speeds of B and C particles depend on flow velocities along the whole ICT, including near the inlet.

Increasing  $L_i$ , while keeping  $\bar{v}$  at the outlet the same, requires higher driving pressures, which imply proportionally lower flow rates at the inlet. Thus, guns with longer ICT that we tested did not give an appreciable increase in the particle penetration depths. However, the depths significantly increased when  $D_i$  was expanded from 250 to 530  $\mu\text{m}$ , allowing lower driving pressure. The expansion of ICT might also have reduced negative effects of uncontrolled transverse motion of the particles and inelastic collisions with the walls. Those collisions may be a cause of the wide distributions of the particle penetration depths (Fig.3). Further expansion of ICT proved impractical, though, since it caused reduction of the velocity of the fastest flow which could be diverted to OCT.

The proposed capillary gun is an easily fabricated alternative to Helios gun. In a pilot experiment we shot B particles coated with GFP expressing reporter plasmid (gWIZ; Aldevron, Fargo, ND) into 293T/17 cells. After 4 hours, we clearly observed fluorescence from GFP expression in a number of cells. The capillary gun gives large penetration depths for small particles without damaging the surfaces of even the softest agarose gels. It can be inserted into openings down to 2.5 mm in size and selectively target small areas. So, it may find applications in medicine and live animal biology. A large fraction of the particles is delivered to a narrow interval of depths, and the characteristic penetration depth is reliably controlled by tailoring the shooting distance. The possibility to estimate and control the speed of the particles makes the gun a promising tool to study microscopic mechanical properties of soft materials.

We are very grateful to David Schultz and Jim Glass from Seashell Co. for multiple useful discussions, encouragement and help with the measurements.

- 1 T.M. Klein, E.D. Wolf, R. Wu, and J.C. Sanford, *Nature* **327**, 70 (1987).  
2 L.T. Pecorino and D.C Lo, *Current Biology* **2**, 30 (1992).  
3 D.C. Lo, A.K. McAllister, and L.C. Katz, *Neuron* **13**, 1263 (1994).  
4 P. Kettunen, J. Demas, C. Lohmann, N. Kasthuri, Y. Gong, R. O.L. Wong, and  
5 W.B. Gan, *J. Neurosci. Methods* **119**, 37 (2002).  
6 W. B. Gan, J. Grutzendler, W.T. Wong, R.O. Wong, and J.W. Lichtman, *Neuron*  
7 **27**, 219 (2000).  
8 J. A. O'Brien, M. Holt, G. Whiteside, S.C. Lummis, and M.H. Hastings, *J*  
9 *Neurosci Methods* **112**, 57 (2001).  
H. Lorenz, M. Despont, N. Fahrni, J. Brugger, P. Vettiger, and P. Renaud,  
*Sensors and Actuators A* **64**, 33 (1998).  
D. J. Tritton, *Physical Fluid Dynamics*. (Oxford University Press, New York,  
1988).  
M. Sherman, *Journal of Fluids Engineering-Transactions of the Asme* **114**, 601  
(1992).

### Figure captions.

Fig.1 Schematic drawing showing the design and operation of the capillary gun with microphotographs of a concentric pinion and the end cap.

Fig.2 Dark field microphotographs of a 3% agarose gel with particles B fired from the capillary gun, (a)-(c), and Helios gun at 175 psi, (d)-(f). The image planes are at the gel surface, (a) and (d), at depth 35  $\mu\text{m}$  into the gel, (b) and (e), and 55  $\mu\text{m}$  into the gel, (c) and (f).

Fig.3 Distributions of penetration depths of particles A, B and C fired into a 3% gel. The solid line is for the capillary gun. The dashed and dotted lines are for Helios gun at pressures of 175 and 120 psi, respectively. **Inset:** Characteristic penetration depth,  $d$ , as a function of shooting distance,  $h$ , for particles A, B and C. Circles, crosses and pluses are for shooting through air, He and H<sub>2</sub>, respectively, with  $h$  multiplied by  $\eta_{\text{He}} / \eta_a$  and  $\eta_{\text{H}} / \eta_a$  in the two latter cases.

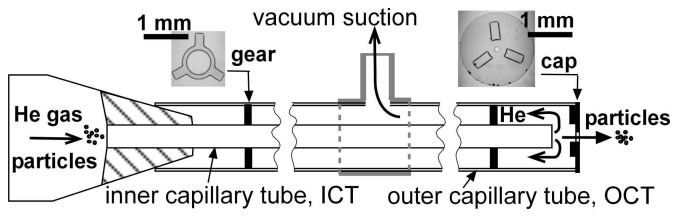


Fig.1

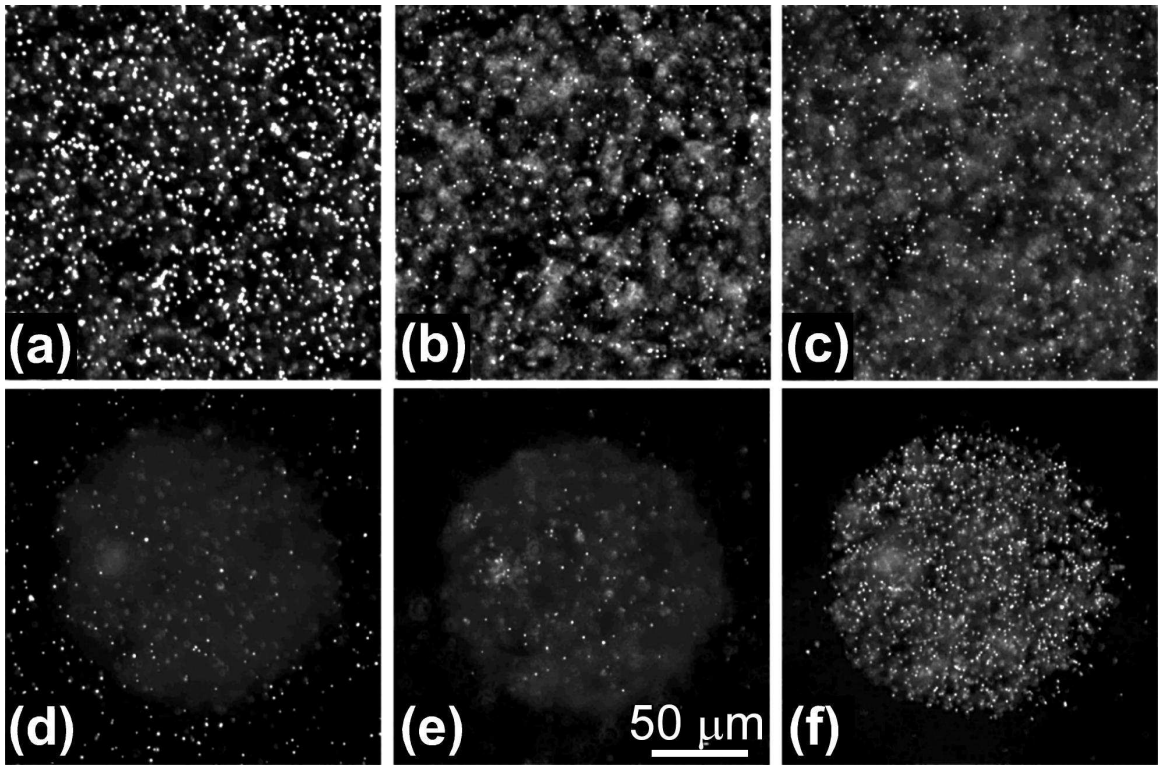


Fig.2

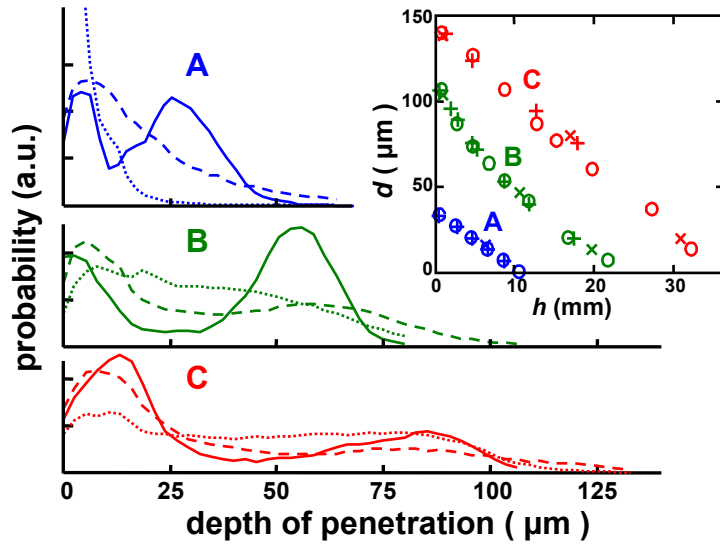


Fig.3